High-dimensional theory of the glass transition revisited: hopping and local defects

Harukuni Ikeda[1,*] and Francesco Zamponi[2]

[1] *Yukawa Institute for Theoretical Physics, Kyoto University, Kyoto 606-8502, Japan*
[2] *Dipartimento di Fisica, Sapienza Università di Roma, P.le Aldo Moro 5, 00185 Rome, Italy*

(Dated: October 15, 2026)

The replicated liquid theory provides a microscopic mean-field description of the glass transition by combining the density functional theory of liquids with the replica method originally developed for spin glasses. In the conventional replica liquid theory, a glassy state is described by assuming that particles in different replicas undergo vibrational motion around common centers of mass, thereby forming molecules that contain one particle from every replica. Here we revisit this assumption by allowing each molecule to contain only a subset of replicas. This generalized formulation describes particle-level replica mismatches, which may be associated with non-vibrational motions such as particle hopping. We apply the theory to high-dimensional hard and harmonic spheres, where the mean-field description is expected to become exact. For hard spheres, replica mismatches destabilize the glassy metastable state and shift the dynamical transition to a significantly higher packing fraction, while leaving the leading thermodynamic glass transition unchanged. The resulting transition density agrees, at leading order in high dimensions, with the recent rigorous lower bound for random sphere packings obtained by Campos, Jenssen, Michelen, and Sahasrabudhe by using a discretized version of greedy Random Sequential Absorption, suggesting an algorithmic interpretation of the transition: grandcanonical dynamics is more efficient in high dimensional spaces than canonical one. For harmonic spheres at finite temperature, the glassy state contains a finite replica-mismatch fraction even at the thermodynamic ideal-glass transition, thereby shifting the transition point from that predicted by the conventional replica ansatz.

arXiv:2607.26793v2 [cond-mat.dis-nn] 14 Oct 2026

CONTENTS

I. Introduction 2

II. Theory 3
A. Sketch of the framework 3
B. Molecular dissociation construction 3
C. Replicated free-energy functional 4
D. Gaussian molecular ansatz 5
E. High-dimensional harmonic spheres 6
F. Binomial ansatz and configurational entropy 7

III. Results 8
A. Hard spheres 8
B. Harmonic spheres at finite temperature 9
C. Replica-mismatch fraction at low temperature 10
D. Comparison with the conventional theory 11

IV. Summary and discussion 12
A. Summary 12
B. Dynamical interpretation 13
C. Localized excitations 13
D. Perspectives 13

Acknowledgments 14

A. Heuristic summary of Campos *et al.* 14

B. More general ansatz 15

* harukuni.ikeda@yukawa.kyoto-u.ac.jp

C. Hard-core model on random graphs in the large-degree limit 17
1. Settings 17
2. Replica free energy 17
3. Factorized 1RSB ansatz 18
4. Small-α expansion 19
5. Binomial ansatz 20

References 20

I. INTRODUCTION

The glass transition is a long-standing problem in statistical and condensed matter physics. When a liquid is cooled or compressed while avoiding crystallization, its relaxation time and viscosity grow dramatically, until it eventually behaves as an amorphous solid. A central question is whether this phenomenon can be described as the emergence of metastable amorphous states and an associated thermodynamic transition [1–3].

The mean-field scenario of the glass transition was originally developed in solvable spin-glass models, most notably the p-spin spherical model [4, 5]. In this scenario, the free-energy landscape splits, upon cooling, into an exponentially large number of metastable states. The emergence of these states is associated with a dynamical transition [6–10], while the point at which their configurational entropy vanishes is identified with the thermodynamic, or ideal-glass, transition. Although finite-dimensional systems may avoid a sharp dynamical singularity through activated processes, this mean-field picture remains an essential reference point for understanding glassy dynamics and thermodynamics [11–13].

The replica liquid theory provides a microscopic realization of this scenario for structural glasses by combining the replica method developed for spin-glasses and the density functional theory of liquids [8, 14–22]. One introduces replicas of the liquid and describes a metastable glass state by assuming that particles in different replicas are localized around common centers of mass, forming molecules made of replicated particles. The replicated system is then treated as a liquid of these molecules. This theory has been particularly successful for high-dimensional spheres, where the virial expansion becomes controlled and the mean-field description is expected to become exact [8, 21–29].

In the conventional replica liquid theory, each molecule contains one particle from every replica, and the replicated particles are localized around a common center [20–22]. This is similar to an Einstein crystal where each atom in the glass is constrained to be localized around its reference position. It therefore excludes particle-level mismatches, where some particles do not form replicated molecules with other replicas. Here we revisit the theory by allowing each molecule to contain only a subset of replicas, leading to fluctuations of molecular sizes. The conventional theory is recovered when all molecules contain all replicas.

There are two main motivations for introducing this extension. The first comes from high-dimensional sphere packing. Recent mathematical progress has established a rigorous lower bound for random sphere packings whose density is significantly higher than the dynamical transition predicted by the conventional replica liquid theory [30]. The fact that this bound is obtained by proving convergence of a discretized version of random sequential absorption, i.e. of a greedy algorithm, suggests that the conventional replica molecular ansatz may underestimate the dynamical transition point. The second motivation comes from numerical simulations of glass forming models, where localized excitations and hopping-like rearrangements have been observed even inside the ideal-glass phase [31–33]. This suggests that an ideal glass should not necessarily be represented by a purely vibrational state in which all replicated particles remain localized around common molecular centers.

In the following, we call "conventional replica theory" that in which each molecule contains one atom of each replica, and "dissociation replica theory" that in which molecules can dissociate. We formulate the dissociation theory and apply it to high-dimensional hard and harmonic spheres. For hard spheres, molecular-size fluctuations destabilize the conventional metastable glass solution and shift the dynamical transition to a significantly higher packing fraction. The shifted transition density agrees, at leading order in high dimensions, with the recent lower bound for random sphere packings obtained by Campos *et al.* [30]. This agreement suggests that the transition may have an algorithmic interpretation, corresponding to the density scale accessible by grandcanonical random packing procedures in which particle number is not conserved. Surprisingly, such procedures would then be more efficient in high dimensions than canonical one, due to the large amount of void space that characterizes high-dimensional sphere packings. For harmonic spheres at finite temperature, the dissociation theory predicts that the glassy solution contains a finite replica-mismatch fraction. This fraction becomes exponentially small at low temperature, but remains finite at the thermodynamic ideal-glass transition point within the present theory. Consequently, the conventional full-replica molecular ansatz overestimates the configurational entropy.

The rest of the paper is organized as follows. In Section II we first give a schematic overview of the molecular dissociation construction, and we then formulate the replica liquid theory with molecular dissociation and derive the corresponding free-energy functional. In Sec. III, we apply the theory to high-dimensional hard and harmonic spheres, and analyze the dynamical and thermodynamic glass transitions. Section IV summarizes the results and discusses their implications. Technical details and connections to independent-set problems on random graphs are given in the Appendices.

II. THEORY

A. Sketch of the framework

We first give a schematic overview of the framework before presenting the formal derivation. Figure 1 illustrates the molecular construction in the conventional replica liquid theory and in the present dissociation theory for $m = 2$ and $m = 3$ replicas.

In the conventional replica liquid theory, a glassy metastable state is described by replicated molecules. Each molecule contains one particle from every replica, and the particles in the molecule are localized around a common molecular center. Thus, for $m = 2$, every molecule is a two-replica pair, while for $m = 3$, every molecule is a three-replica triplet, as shown in the left panels of Fig. 1. Because within replica theory distinct replicas physically correspond to pairs of independent configurations belonging to the same metastable state [18], this ansatz physically corresponds to the assumption that within each metastable glass, an atom always remains near its initial position, and no hopping is possible.

In the present work, we generalize this construction by allowing a molecule to contain only a subset of replicas. For $m = 2$, molecules can therefore be either two-replica pairs or single-replica objects. For $m = 3$, molecules can be triplets, two-replica pairs, or single-replica objects. This introduces fluctuations in the molecular size and provides a simple way to describe particle-level mismatches between replicas within the replica liquid theory framework, physically corresponding to hopping processes within the metastable glass phase, which allow atoms to hop away from the original position. The conventional replica liquid theory is recovered when all molecules contain all replicas.

In the following, we formulate this idea quantitatively. We introduce a binary molecular label specifying which replicas participate in each molecule, construct the corresponding replicated free-energy functional, and analyze the consequences of molecular dissociation for high-dimensional hard and harmonic spheres.

B. Molecular dissociation construction

In this section, we formulate the replica liquid theory with fluctuating molecular sizes. Following the standard strategy of the replica liquid theory, we introduce m replicas of each atom [18, 20, 21]. In the conventional theory, each molecule contains one particle from every replica. Here we relax this constraint and allow a molecule to contain only a subset of replicas. We thus introduce generalized replicated molecules that may contain only a subset of replicas. We then derive the corresponding free-energy functional within the second-virial approximation and impose a Gaussian molecular ansatz. Finally, we take the high-dimensional limit for harmonic spheres and introduce a one-parameter binomial ansatz, from which the configurational entropy is obtained.

We label the type of a molecule by a binary vector

$$\overline{\mu} = \{\mu^1, \mu^2, \cdots, \mu^m\}, \tag{1}$$

where $\mu^a = 1$ means that the molecule contains a particle from replica a, while $\mu^a = 0$ means that it does not. The molecular size in replica space is

$$|\overline{\mu}| = \sum_{a=1}^{m} \mu^a. \tag{2}$$

The empty molecule, $|\overline{\mu}| = 0$, is excluded. We denote by $N(\overline{\mu})$ the number of molecules of type $\overline{\mu}$, and write

$$N(\overline{\mu}) = N g(\overline{\mu}). \tag{3}$$

The coefficients $g(\overline{\mu})$ are not normalized as probabilities. The normalization condition is imposed by requiring that each replica contains exactly N particles:

$$N = \sum_{\overline{\mu}} N(\overline{\mu})\mu^a, \qquad a = 1, \cdots, m. \tag{4}$$

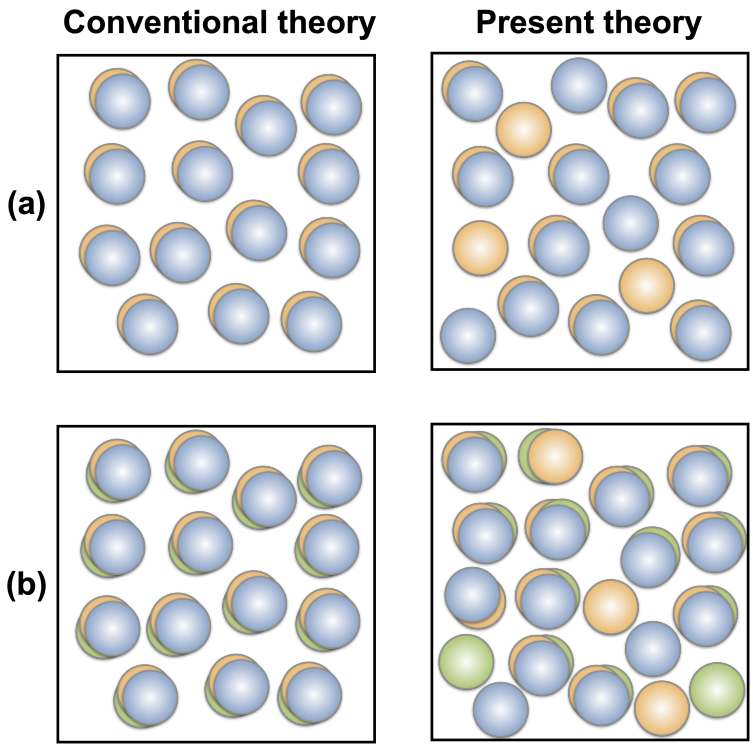


FIG. 1. Schematic illustration of the conventional replica liquid theory and of the molecular dissociation construction introduced in this work. Panel (a) shows the case $m = 2$, and panel (b) the case $m = 3$. Disks of different colors denote particles in different replicas. In the conventional theory (left panels), every molecule contains one particle from each replica. In the present theory (right panels), a molecule may contain any non-empty subset of replicas. Thus, for $m = 2$, there are $2^2 - 1 = 3$ possible molecular types, $(\mu^1, \mu^2) = (1, 1), (1, 0), (0, 1)$, while for $m = 3$ there are $2^3 - 1 = 7$ possible molecular types, $(\mu^1, \mu^2, \mu^3) = (1, 1, 1), (1, 1, 0), (1, 0, 1), (0, 1, 1), (1, 0, 0), (0, 1, 0), (0, 0, 1)$.

Equivalently,

$$1 = \sum_{\overline{\mu}} g(\overline{\mu})\mu^a. \tag{5}$$

In the following, we impose replica symmetry and assume that $g(\overline{\mu})$ depends only on the molecular size $|\overline{\mu}|$:

$$g(\overline{\mu}) = g_{|\overline{\mu}|}. \tag{6}$$

The normalization condition then becomes

$$1 = \sum_{k=1}^{m} \binom{m-1}{k-1} g_k. \tag{7}$$

The conventional replica liquid theory is recovered by the fixed-size choice $g_k = \delta_{km}$, whereas the completely unbound liquid corresponds to $g_k = \delta_{k1}$.

C. Replicated free-energy functional

Let

$$\overline{x} = \{x^1, \cdots, x^m\}, \qquad \overline{x}_{\overline{\mu}} = \{x^a\}_{a:\mu^a=1}. \tag{8}$$

The interaction between two molecules of types $\overline{\mu}$ and $\overline{\nu}$ is defined as

$$V_{\overline{\mu},\overline{\nu}}(\overline{x}_{\overline{\mu}}, \overline{y}_{\overline{\nu}}) = \sum_{a=1}^{m} \mu^a \nu^a v(x^a - y^a), \tag{9}$$

where $v(x)$ is the atomic pair potential. Thus, an interaction exists only when both molecules contain particles belonging to the same replica. We consider the grand-canonical ensemble of the generalized molecular system,

$$\Xi = \sum_{N_{\rm mol}=0}^{\infty} \frac{1}{N_{\rm mol}!} \left(\prod_{i=1}^{N_{\rm mol}} \sum_{\overline{\mu}_i : |\overline{\mu}_i|>0} \int d\overline{x}^i_{\overline{\mu}_i} \right) \exp\left[-\beta \sum_i \phi_{\overline{\mu}_i}(\overline{x}^i_{\overline{\mu}_i}) - \beta \sum_{i<j} V_{\overline{\mu}_i,\overline{\mu}_j}(\overline{x}^i_{\overline{\mu}_i}, \overline{x}^j_{\overline{\mu}_j}) \right], \tag{10}$$

where $N_{\rm mol} = \sum_{|\overline{\mu}|>0} N(\overline{\mu})$ is the total number of molecules. The auxiliary field $\phi_{\overline{\mu}}(\overline{x}_{\overline{\mu}})$ is conjugate to the density field of molecules of type $\overline{\mu}$:

$$\rho_{\overline{\mu}}(\overline{x}_{\overline{\mu}}) = -\frac{1}{\beta} \frac{\delta \log \Xi}{\delta \phi_{\overline{\mu}}(\overline{x}_{\overline{\mu}})}. \tag{11}$$

Performing the Legendre transform and retaining terms up to the second virial order [17, 21, 22], we obtain

$$\begin{aligned} -\beta F = & \sum_{\overline{\mu}:|\overline{\mu}|>0} \int d\overline{x}_{\overline{\mu}}\, \rho_{\overline{\mu}}(\overline{x}_{\overline{\mu}}) \left[1 - \log \rho_{\overline{\mu}}(\overline{x}_{\overline{\mu}})\right] \\ & + \frac{1}{2} \sum_{\overline{\mu},\overline{\nu}:|\overline{\mu}|,|\overline{\nu}|>0} \int d\overline{x}_{\overline{\mu}} d\overline{y}_{\overline{\nu}}\, \rho_{\overline{\mu}}(\overline{x}_{\overline{\mu}}) \rho_{\overline{\nu}}(\overline{y}_{\overline{\nu}}) f_{\overline{\mu}\overline{\nu}}(\overline{x}_{\overline{\mu}}, \overline{y}_{\overline{\nu}}), \end{aligned} \tag{12}$$

where the Mayer function is

$$f_{\overline{\mu}\overline{\nu}}(\overline{x}_{\overline{\mu}}, \overline{y}_{\overline{\nu}}) = \exp\left[-\beta V_{\overline{\mu},\overline{\nu}}(\overline{x}_{\overline{\mu}}, \overline{y}_{\overline{\nu}})\right] - 1. \tag{13}$$

In high dimensions, higher-order virial terms are negligible for the glass transition of hard and soft spheres [21, 22]. They could possibly be included and partially resummed to obtain approximate finite-dimensional theories [21, 34].

D. Gaussian molecular ansatz

We now impose a Gaussian ansatz for molecules of each type [21]:

$$\rho_{\overline{\mu}}(\overline{x}_{\overline{\mu}}) = \rho g_{|\overline{\mu}|} \int dX \prod_{a:\mu^a=1} \gamma_A(x^a - X), \qquad \gamma_A(r) = \frac{1}{(2\pi A)^{d/2}} \exp\left(-\frac{r^2}{2A}\right). \tag{14}$$

Here X is the molecular center and A is the cage size. Substituting Eq. (14) into the ideal-gas part of Eq. (12), we obtain the ideal contribution to the free energy per particle:

$$\begin{aligned} -\beta f^{\rm id} = & \sum_{k=1}^{m} \binom{m}{k} g_k \left(1 - \log\rho - \log g_k\right) \\ & - \sum_{k=2}^{m} \binom{m}{k} g_k \int \frac{d\overline{x}_k}{V} \rho_k(\overline{x}_k) \log \rho_k(\overline{x}_k), \end{aligned} \tag{15}$$

where

$$\rho_k(\overline{x}_k) = \int dX \prod_{a=1}^{k} \gamma_A(x^a - X). \tag{16}$$

The Gaussian integral gives [21]

$$\int d\overline{x}_k\, \rho_k(\overline{x}_k) \log \rho_k(\overline{x}_k) = V \left[\frac{d}{2}(1-k)\log(2\pi A) - \frac{d}{2}\log k + \frac{d}{2}(1-k) \right], \tag{17}$$

and hence

$$\begin{aligned} -\beta f^{\rm id} = & \sum_{k=1}^{m} \binom{m}{k} g_k \left(1 - \log\rho - \log g_k\right) \\ & - \sum_{k=2}^{m} \binom{m}{k} g_k \left[\frac{d}{2}(1-k)\log(2\pi A) - \frac{d}{2}\log k + \frac{d}{2}(1-k) \right]. \end{aligned} \tag{18}$$

We next compute the interaction term. If two molecules have no common replica, namely if $\mu^a\nu^a = 0$ for all a, then $f_{\overline{\mu}\overline{\nu}} = 0$. Thus, only molecules sharing at least one replica contribute. Consider a molecule $\overline{\mu}$ of size $k = |\overline{\mu}|$. By replica symmetry, we may assume that the first k components of $\overline{\mu}$ are equal to one. For the second molecule $\overline{\nu}$, let ℓ be the number of replicas shared with $\overline{\mu}$, and let s be the number of replicas contained in $\overline{\nu}$ but not in $\overline{\mu}$. Then $|\overline{\nu}| = \ell + s$, with $1 \le \ell \le k$ and $0 \le s \le m - k$. After integrating over the coordinates that are not shared, the excess free energy becomes

$$-\beta f^{\rm ex} = \frac{\rho}{2}\sum_{k=1}^{m}\binom{m}{k} g_k \sum_{\ell=1}^{k}\sum_{s=0}^{m-k}\binom{k}{\ell}\binom{m-k}{s} g_{\ell+s}\int dr\,\left[q_A(r)^\ell - 1\right], \tag{19}$$

where

$$q_A(r) = \int du\,\gamma_{2A}(r-u)\exp[-\beta v(u)]. \tag{20}$$

Equations (18) and (19) give the free-energy functional for an arbitrary replica-symmetric molecular-size distribution $\{g_1, \cdots, g_m\}$.

E. High-dimensional harmonic spheres

We now specialize the theory to high-dimensional harmonic spheres. The pair interaction is

$$v(r) = \begin{cases} \dfrac{\kappa}{2}\left(1 - \dfrac{r}{D}\right)^2, & r \le D, \\ 0, & r > D, \end{cases} \tag{21}$$

where D is the particle diameter and κ is the stiffness. The packing fraction is

$$\varphi = \rho v_d \left(\frac{D}{2}\right)^d, \qquad v_d = \frac{\pi^{d/2}}{\Gamma(d/2+1)}, \tag{22}$$

where v_d is the volume of a d-dimensional unit sphere. For reasons that will become clear in the following, we focus on the density scale $\varphi \sim 2^{-d} d\log d$ and introduce

$$\widetilde{\varphi} = \frac{\varphi}{2^{-d} d\log d}, \qquad \hat{A} = \frac{d^2 A}{D^2}, \qquad \tilde{\beta} = \frac{\beta\kappa}{d^2}. \tag{23}$$

At this scale,

$$\log\rho = \frac{d}{2}\log d + o(d\log d), \qquad d\log A = -2d\log d + o(d\log d). \tag{24}$$

Keeping only the leading $O(d\log d)$ terms in Eq. (18), we find

$$-\beta f^{\rm id} \simeq \frac{d\log d}{2}\sum_{k=1}^{m}\binom{m}{k} g_k(1-2k) = \frac{d\log d}{2}\left[\sum_{k=1}^{m}\binom{m}{k} g_k - 2m\right]. \tag{25}$$

The interaction term is controlled by

$$\rho\int dr\,\left[q_A(r)^\ell - 1\right]. \tag{26}$$

At the scale of the dynamical transition of the conventional molecular ansatz, $\varphi = O(2^{-d}d)$, this term is only $O(d)$, and is therefore subleading compared with the $O(d\log d)$ ideal contribution in the present generalized variational space. This motivates the higher density scale $\varphi \sim 2^{-d} d\log d$, where the ideal and interaction terms compete. At this density scale, the cage size vanishes asymptotically $\hat{A} = O(1/\log d)$ [21], and we may approximate

$$q_A(r) \simeq e^{-\beta v(r)} \tag{27}$$

at leading order. Using the standard high-dimensional change of variables [22]

$$r = D\left(1+\frac{h}{d}\right), \tag{28}$$

we obtain

$$\begin{aligned}\rho\int dr\ \left[q_A(r)^\ell - 1\right] &\simeq \rho\int dr\ \left[e^{-\ell\beta v(r)}-1\right]\\ &= \rho\Omega_d\int_0^\infty dr\, r^{d-1}\left[e^{-\ell\beta v(r)}-1\right]\\ &= \frac{\rho\Omega_d D^d}{d}\int_{-\infty}^\infty dh\left(1+\frac{h}{d}\right)^{d-1}\left[e^{-\ell\tilde\beta\tilde v(h)}-1\right]\\ &\simeq 2^d\varphi\int_{-\infty}^0 dh\, e^h\left[e^{-\ell\tilde\beta\tilde v(h)}-1\right],\end{aligned} \tag{29}$$

where

$$\tilde v(h) = \frac{h^2}{2}. \tag{30}$$

Therefore, Eq. (19) becomes

$$-\beta f^{\rm ex} \simeq d\log d\,\frac{\widetilde\varphi}{2}\sum_{k=1}^m\binom{m}{k}g_k\sum_{\ell=1}^k\sum_{s=0}^{m-k}\binom{k}{\ell}\binom{m-k}{s}g_{\ell+s}\int_{-\infty}^0 dh\, e^h\left[e^{-\ell\tilde\beta\tilde v(h)}-1\right]. \tag{31}$$

Combining Eqs. (25) and (31), the leading high-dimensional free energy is

$$\begin{aligned}-\beta f = {}& \frac{d\log d}{2}\left[\sum_{k=1}^m\binom{m}{k}g_k - 2m\right]\\ &+ d\log d\,\frac{\widetilde\varphi}{2}\sum_{k=1}^m\binom{m}{k}g_k\sum_{\ell=1}^k\sum_{s=0}^{m-k}\binom{k}{\ell}\binom{m-k}{s}g_{\ell+s}\int_{-\infty}^0 dh\, e^h\left[e^{-\ell\tilde\beta\tilde v(h)}-1\right].\end{aligned} \tag{32}$$

In the zero-temperature limit, $\tilde\beta\to\infty$, this expression reduces to the corresponding hard-sphere free energy. The ideal-glass transition density predicted by the conventional molecular ansatz corresponds to $\widetilde\varphi = 1$ at leading order [21]. Interestingly, the free energy of hard spheres agrees with that of the hard-core model on random graphs in the large degree limit, see Appendix C.

F. Binomial ansatz and configurational entropy

To obtain explicit results, we now restrict the molecular-size distribution to the binomial form

$$g_k = x^{k-1}(1-x)^{m-k}, \qquad 0\le x\le 1. \tag{33}$$

This ansatz satisfies the normalization condition (7). The limits $x=0$ and $x=1$ correspond, respectively, to the unbound liquid ansatz $g_k=\delta_{k1}$ and the conventional full-replica molecular ansatz $g_k=\delta_{km}$.

The parameter x has a direct interpretation as an inter-replica overlap. To see this, define

$$Q_{ab} \equiv \frac{1}{N}\sum_{i=1}^{N_{\rm mol}}\left\langle \mu_i^a\mu_i^b\theta\left(\sigma-|x_i^a-x_i^b|\right)\right\rangle, \qquad a\neq b, \tag{34}$$

where σ is a small microscopic length. In the high-dimensional regime considered above, the cage size vanishes at leading order, and the Heaviside factor is equal to one when replicas a and b belong to the same molecule. Thus,

$$Q_{ab} = \frac{1}{N}\sum_{i=1}^{N_{\rm mol}}\left\langle\mu_i^a\mu_i^b\right\rangle = \sum_{\overline\mu} g(\overline\mu)\mu^a\mu^b = \sum_{k=2}^m\binom{m-2}{k-2}g_k = x, \tag{35}$$

suggesting that x is the overlap between different replicas within the binomial ansatz. It is also useful to define the replica-pair mismatch fraction

$$c \equiv \frac{1}{N}\sum_{i=1}^{N_{\rm mol}} \left\langle \mu_i^a(1-\mu_i^b)\right\rangle = 1-x. \tag{36}$$

This quantity measures the fraction of particles in replica a that are not bound to their counterparts in replica b.

Using Eq. (33), the ideal contribution becomes

$$-\beta f^{\rm id} = \frac{d\log d}{2}\left[\frac{1-(1-x)^m}{x} - 2m\right], \tag{37}$$

and the excess contribution becomes

$$-\beta f^{\rm ex} = \frac{d\log d}{2}\widetilde{\varphi}\int_{-\infty}^{0} dh\, e^h \frac{\left[1+\left(e^{-\tilde{\beta}\tilde{v}(h)}-1\right)x^2\right]^m - 1}{x^2}. \tag{38}$$

We now compute the configurational entropy by analytically continuing the replicated free energy to real m. Let

$$s(m,x) \equiv \frac{-\beta f(m,x)}{d\log d/2}. \tag{39}$$

The rescaled configurational entropy is obtained from the Monasson's method [18]

$$\tilde{\Sigma}(x) \equiv \frac{\Sigma(x)}{d\log d/2} = \left[s(m,x) - m\partial_m s(m,x)\right]_{m=1}, \tag{40}$$

where the derivative is taken at fixed x. This gives

$$\tilde{\Sigma}(x) = A(x) - \widetilde{\varphi}\int_{-\infty}^{0} dh\, e^h\, B(h) A\left(B(h)x^2\right), \tag{41}$$

where

$$A(x) = 1 + \frac{1-x}{x}\log(1-x), \qquad B(h) = 1 - e^{-\tilde{\beta}\tilde{v}(h)}. \tag{42}$$

This expression is the starting point for the analysis of the dynamical and thermodynamic glass transitions in the next section.

III. RESULTS

A. Hard spheres

We first consider the hard-sphere limit, $\tilde{\beta}\to\infty$. In this limit, $B(h)\to 1$, and Eq. (41) reduces to

$$\tilde{\Sigma}(x) = A(x) - \widetilde{\varphi}A(x^2). \tag{43}$$

Figure 2 shows the rescaled configurational entropy $\tilde{\Sigma}(x)$. For $\widetilde{\varphi}<1/2$, $\tilde{\Sigma}(x)$ is monotonic and its minimum is located at $x=0$, corresponding to the liquid state. For $\widetilde{\varphi}>1/2$, a glassy minimum appears at the boundary $x=1$.

This boundary minimum is identified from the behavior near $x=1$. For $1-x\ll 1$, Eq. (43) gives

$$\frac{\partial\tilde{\Sigma}}{\partial x} \simeq -(1-2\widetilde{\varphi})\log(1-x). \tag{44}$$

Since $\log(1-x)<0$, the endpoint $x=1$ becomes a local minimum when $\widetilde{\varphi}>1/2$. Thus the dynamical transition occurs at

$$\widetilde{\varphi}_d = \frac{1}{2}, \qquad \varphi_d = \frac{2^{-d}d\log d}{2}. \tag{45}$$

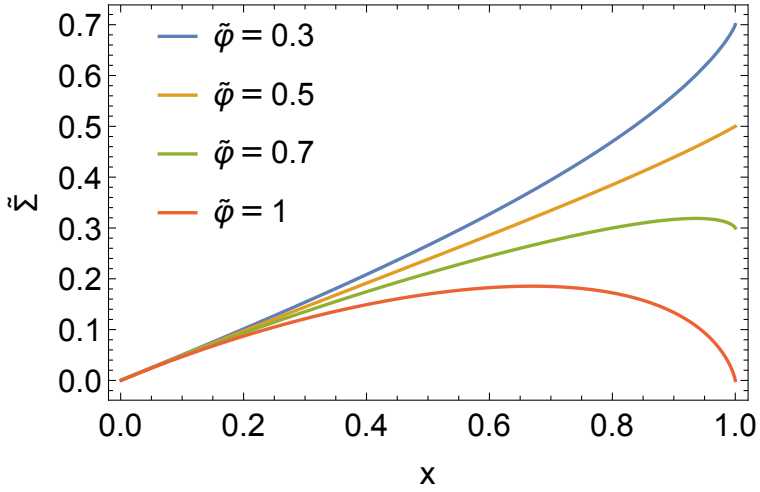


FIG. 2. Configurational entropy of hard spheres. For $\widetilde{\varphi} < 1/2$, $\tilde{\Sigma}(x)$ is monotonic and has its minimum at $x = 0$. For $\widetilde{\varphi} > 1/2$, a boundary minimum appears at $x = 1$. This minimum becomes the global minimum at $\widetilde{\varphi} = 1$.

This transition density agrees, at leading order in high dimensions, with the recent rigorous lower bound for random sphere packings obtained by Campos, Jenssen, Michelen, and Sahasrabudhe [30]. This agreement suggests that the shifted dynamical transition may have an algorithmic interpretation: it gives the density scale accessible by constructive random packing procedures that do not conserve the particle number. We discuss this connection in more detail in Appendix A.

The boundary glassy minimum becomes the global minimum at $\widetilde{\varphi} = 1$. Therefore, the ideal-glass transition occurs at

$$\widetilde{\varphi}_K = 1, \qquad \varphi_K = 2^{-d} d \log d, \tag{46}$$

which agrees with the leading high-dimensional result of the conventional replica liquid theory [21]. Thus, for hard spheres, molecular-size fluctuations shift the dynamical transition but leave the leading ideal-glass transition density unchanged.

B. Harmonic spheres at finite temperature

We next consider harmonic spheres at finite temperature. In contrast to the hard-sphere limit, the glassy minimum is no longer located at $x = 1$. As shown in Fig. 3, the metastable glassy solution appears at an interior point $x_{\min} < 1$. This means that the glassy state contains a finite replica-pair mismatch fraction at finite temperature.

The position of the glassy minimum is determined by the stationarity condition

$$\frac{\partial \tilde{\Sigma}(x)}{\partial x} = A'(x) - \widetilde{\varphi} \int_{-\infty}^{0} dh\, e^h\, 2xB(h)^2 A'\left(B(h)x^2\right) = 0. \tag{47}$$

Solving the stationarity condition for $\widetilde{\varphi}$, one obtains

$$\widetilde{\varphi}(x) = \frac{A'(x)}{\int_{-\infty}^{0} dh\, e^h\, 2xB(h)^2 A'(B(h)x^2)}. \tag{48}$$

The dynamical transition is the spinodal at which a glassy stationary point first appears, and is therefore given by

$$\widetilde{\varphi}_d = \min_{0<x<1} \widetilde{\varphi}(x) = \min_{0<x<1} \frac{A'(x)}{\int_{-\infty}^{0} dh\, e^h\, 2xB(h)^2 A'(B(h)x^2)}. \tag{49}$$

The thermodynamic ideal-glass transition is obtained when the value of $\tilde{\Sigma}(x)$ at the secondary minimum reaches zero. Equivalently, it is the lowest density for which $\tilde{\Sigma}(x) = 0$ has a solution for $x > 0$. This gives

$$\widetilde{\varphi}_K = \min_{0<x<1} \frac{A(x)}{\int_{-\infty}^{0} dh\, e^h\, B(h) A\left(B(h)x^2\right)}. \tag{50}$$

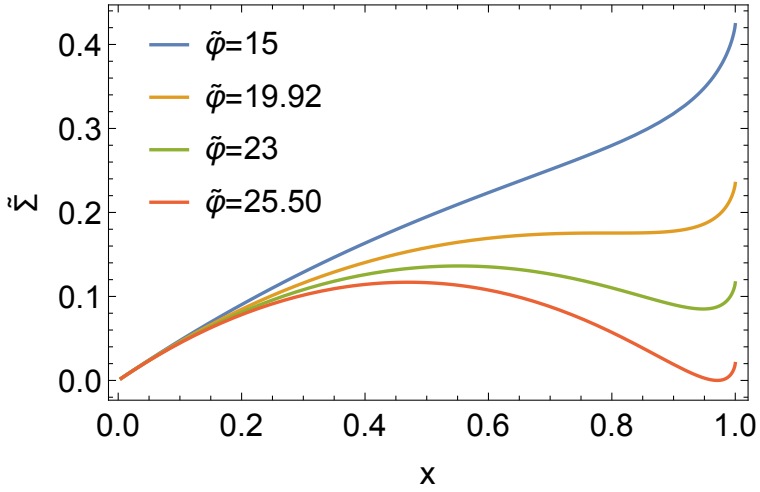


FIG. 3. Configurational entropy of harmonic spheres for $\tilde{\beta} = 0.2$. The glassy minimum appears at $x_{\min} < 1$. The dynamical and thermodynamic transition points are $\widetilde{\varphi}_d \simeq 19.92$ and $\widetilde{\varphi}_K \simeq 25.50$, respectively.

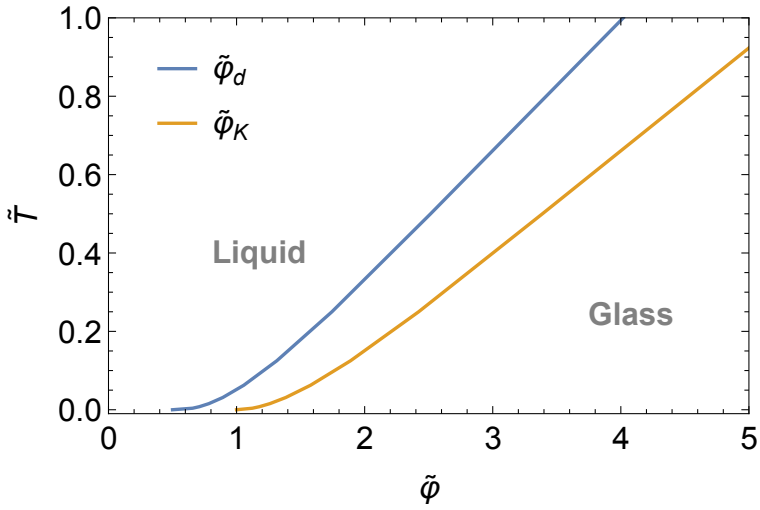


FIG. 4. Phase diagram of high-dimensional harmonic spheres, where $\tilde{T} = \tilde{\beta}^{-1}$.

Equations (49) and (50) allow us to compute the dynamical and thermodynamic transition points very easily.

Figure 4 shows the resulting phase diagram. The region between $\widetilde{\varphi}_d$ and $\widetilde{\varphi}_K$ corresponds to a metastable glassy phase with a finite replica-mismatch fraction. At $\widetilde{\varphi}_K$, the configurational entropy of this glassy minimum vanishes, $\tilde{\Sigma}(x_{\min}) = 0$.

C. Replica-mismatch fraction at low temperature

We now analyze the low-temperature behavior of the replica-pair mismatch fraction,

$$c = 1 - x_{\min}. \tag{51}$$

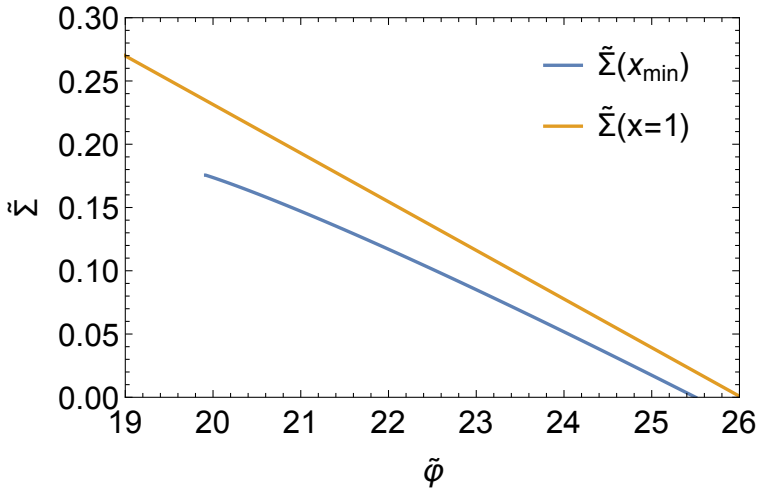


FIG. 5. Configurational entropy of harmonic spheres at $\tilde{\beta} = 0.2$, evaluated at $x_{\min}$ and $x = 1$. The conventional replica liquid theory, corresponding to $x = 1$, overestimates the configurational entropy.

At low temperature, c is small. Setting $x = 1 - c$ with $c \ll 1$ and using $A'(x) \simeq -\log c$, the stationarity condition (47) gives

$$\begin{aligned} \log c &\simeq 2\widetilde{\varphi} \int_{-\infty}^{0} dh\, e^h \log\left(e^{-\tilde{\beta}\tilde{v}(h)} + 2c\right) \\ &\simeq -2\widetilde{\varphi}\tilde{\beta} \int_{-\infty}^{0} dh\, e^h \min\left[\frac{h^2}{2}, -\frac{\log c}{\tilde{\beta}}\right]. \end{aligned} \tag{52}$$

Introducing

$$\lambda = -\frac{\log c}{\tilde{\beta}}, \tag{53}$$

Eq. (52) becomes

$$\widetilde{\varphi} = G(\lambda), \qquad G(\lambda) \equiv \frac{\lambda}{2\int_0^\infty dt\, e^{-t} \min\left[\frac{t^2}{2}, \lambda\right]} = \frac{\lambda}{2\left[1 - (1+\sqrt{2\lambda})e^{-\sqrt{2\lambda}}\right]}. \tag{54}$$

The function $G(\lambda)$ is defined for $\lambda \geq 0$ and satisfies $G(0) = 1/2$. Therefore, for $\widetilde{\varphi} \geq 1/2$, Eq. (54) admits a finite solution $\lambda(\widetilde{\varphi})$. The mismatch fraction then obeys the Arrhenius form

$$c \sim \exp\left[-\tilde{\beta}\lambda(\widetilde{\varphi})\right]. \tag{55}$$

Thus, the replica-mismatch fraction is exponentially suppressed at low temperature. Nevertheless, the optimized glassy solution still has a finite mismatch fraction at the thermodynamic glass transition point of the harmonic sphere system.

D. Comparison with the conventional theory

Finally, we compare the results obtained including molecular dissociation with the conventional replica liquid theory. The latter is recovered by setting $x = 1$, namely by imposing that every molecule contains one particle from every replica. Figure 5 compares the configurational entropy evaluated at the optimized value $x_{\min}$ with that evaluated at $x = 1$. Since

$$\tilde{\Sigma}(x_{\min}) < \tilde{\Sigma}(x = 1), \tag{56}$$

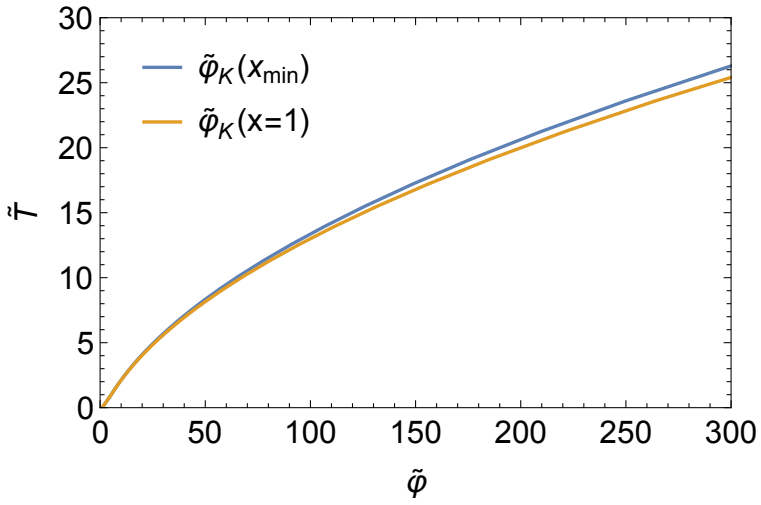


FIG. 6. Thermodynamic glass transition point of harmonic spheres. The optimized result at $x_{\min}$ is compared with the conventional replica liquid theory at $x = 1$, which overestimates the transition density, or equivalently underestimates the transition temperature.

the conventional molecular ansatz overestimates the configurational entropy of the glass.

This difference shifts the predicted thermodynamic transition point. Figure 6 compares the transition point obtained from the optimized ansatz with that obtained by imposing $x = 1$. Since the full-replica molecular ansatz overestimates the configurational entropy, it also overestimates the transition packing fraction, or equivalently underestimates the transition temperature.

This comparison also clarifies the physical meaning of conventional estimates of the configurational entropy. Conventional numerical estimates usually obtain the configurational entropy by subtracting the vibrational entropy from the total entropy [35–37]. In the language of replica liquid theory, this corresponds to the full-replica molecular ansatz, in which all replicated particles remain bound around common molecular centers and undergo only vibrational motions. As shown above, this ansatz overestimates the configurational entropy and can therefore shift the ideal-glass transition point. This interpretation is consistent with simulations of glass forming systems, where localized excitations are present even inside the ideal-glass phase [31, 33].

IV. SUMMARY AND DISCUSSION

A. Summary

In this work, we revisited the replica liquid theory of the glass transition by relaxing the conventional full-replica molecular ansatz, where each molecule contains one particle from every replica. We generalized this construction by allowing each molecule to contain only a subset of replicas. This introduces fluctuations in the molecular size and provides a simple way to describe particle-level replica mismatches within the replica liquid theory framework. We derived the free-energy functional of this replicated molecular system including dissociation, within the second-virial approximation and applied it to high-dimensional hard and harmonic spheres. In the large-dimensional limit, the theory simplifies considerably. Within the binomial ansatz, the molecular-size distribution is controlled by a single parameter x, which coincides with the overlap between different replicas. For hard spheres, molecular-size fluctuations destabilize the conventional glassy metastable solution and shift the dynamical transition from the conventional scale $O(2^{-d}d)$ to $O(2^{-d}d\log d)$. By contrast, the leading thermodynamic transition density remains unchanged. For harmonic spheres at finite temperature, the glassy metastable state appears at $x < 1$, indicating a finite mismatch fraction between replicas. This mismatch fraction remains finite even at the thermodynamic glass transition, thereby shifting the transition point from that predicted by the conventional full-replica ansatz, even in the high-dimensional limit.

B. Dynamical interpretation

The shifted dynamical transition of hard spheres agrees, at the level of leading high-dimensional asymptotics, with the recent constructive lower bound for random sphere packings obtained by Campos, Jenssen, Michelen, and Sahasrabudhe [30] that, as discussed in more details in Appendix A, is obtained by proving convergence of a properly discretized Random Sequential Absorption (RSA) algorithm. This agreement suggests that the dynamical transition found here may have an algorithmic interpretation: it gives the density scale accessible by constructive random packing procedures that do not conserve particle number, i.e. in which particles can appear and/or disappear. The analogy with hard-core lattice gas problems on random graphs, discussed in Appendix C, supports this interpretation.

More precisely, consider the Monte Carlo dynamics of N particles, each having position x_i and carrying an additional binary degree of freedom $\mu_i \in \{0, 1\}$. When $\mu_i = 0$, particle i is a non-interacting ideal gas particle; when $\mu_i = \mu_j = 1$, then the particles interact with potential $v(x_i - x_j)$. One can consider a dynamics satisfying detailed balance, in which for instance the x_i perform a Langevin dynamics with pair potential $\mu_i \mu_j v(x_i - x_j)$, and from time to time one of the μ_i is flipped with the Metropolis rule, adding a chemical potential that fixes the density of $\mu = 1$. The invariant measure of this system is that of a mixture, but the ideal-gas particles with $\mu = 0$ can be integrated away: the remaining measure is a grand-canonical one for the liquid of particles with $\mu = 1$ and pair potential $v(r)$. The long-time limit of this dynamics can be described using replicas [9, 22] and leads precisely to a replicated partition function of the form (10), after the ideal-gas molecules with $|\overline{\mu}| = 0$ are once again integrated away.

We thus speculate that the dynamical transition $\varphi_d \sim d \log d / 2^{d+1}$ given by the molecular ansatz including dissociation corresponds to a class of dynamics that do not conserve the number of interacting particles, such as the one described above. Instead, standard particle-number-conserving dynamics such as pure Langevin become arrested at much lower density $\varphi \propto d 2^{-d}$, as predicted by the conventional molecular ansatz [21, 22]. The fact that different dynamical rules can give widely different dynamical arrest densities is not surprising, and is well established e.g. in the case of the swap Monte Carlo algorithm [38]. The fact that replica theory, which is based on thermodynamics, can capture these differences is also well understood, because the replicated free energy is a Franz-Parisi potential whose form depends on the choice of the molecular coupling, different choices corresponding to different dynamical rules and hence different dynamical order parameters [39, 40].

Instead, the fact that packing algorithms that do not conserve particle number (such as RSA or grand-canonical Monte Carlo) are more efficient in high dimensions than particle-conserving algorithms such as Langevin, Newtonian, or Monte Carlo dynamics is genuinely surprising, at least to us. We believe that this is due to the peculiar properties of high-dimensional sphere packings, which feature a very diluted, random-graph-like, network of particle contacts immersed in large void regions. Strict particle conservation can lead to jamming in a non-saturated packing with large enough voids, while the possibility to remove and/or add particles can lead to a properly saturated packing where no void can be occupied by an additional sphere.

C. Localized excitations

For harmonic spheres at finite temperature, the glassy solution is located at $x < 1$, rather than at the conventional value $x = 1$. The glassy state therefore contains a finite fraction of mismatch between replicas, which follows the Arrhenius law. The conventional theory restricted to $x = 1$ overestimates the configurational entropy, and therefore gives a finite configurational entropy even at the ideal-glass transition. This interpretation is consistent with computer simulation in randomly pinned systems [41, 42], where the configurational entropy remains finite even inside the ideal-glass phase, due to the contributions of localized excitations [31]. More generally, the existence of localized excitations within the glass is well known [43] and the present approach could be a first step toward including these excitations within mean field theory.

D. Perspectives

Several limitations should be kept in mind. First, most explicit calculations in the main text were performed within the binomial ansatz for g_k. Appendix B shows that the thermodynamic transition is unchanged within a broader class of g_k, but a complete analysis remains an open problem. Second, the present theory is static. In infinite-dimensional particle systems, the dynamical transition obtained from the conventional replica calculation with $x = 1$ is known to coincide with that obtained from Langevin dynamics [9, 10, 22]. This agreement is naturally understood from the fact that activated hopping and cage escape are suppressed in the infinite-dimensional limit [32]. From this viewpoint, the present formulation may be regarded as a static way of incorporating hopping-like local rearrangements through replica mismatches. Developing a dynamical mean field theory that explicitly includes such processes remains an

important open problem, as discussed above. Such a dynamical extension of the present theory may also clarify the relation between mean field theory and the dynamical facilitation scenario [44, 45], where relaxation is controlled by sparse localized excitations. The molecular dissociation mechanism introduced here may be viewed as a static counterpart of such excitations. A theory describing their creation and propagation would provide a possible bridge between replica liquid theory and dynamical facilitation.

ACKNOWLEDGMENTS

We thank P. Charbonneau, L. Cugliandolo, G. Folena, A. Ikeda, M. Jenssen, J. Kurchan, P. Morse, Y. Nishikawa, F. Ricci-Tersenghi, and G. Szamel for useful discussions. This project has received JSPS KAKENHI Grant Numbers 23K13031 and 25H01401.

Appendix A: Heuristic summary of Campos *et al.*

To make the present paper self-contained, we briefly summarize the recent lower bound on high-dimensional sphere packings obtained by Campos, Jenssen, Michelen, and Sahasrabudhe (CJMS) [30]. The purpose of this appendix is not to reproduce their rigorous proof, but to give a heuristic interpretation of the result in a form useful for comparison with the replica liquid theory.

The key idea is to reduce the packing problem to an independent-set problem on a random geometric graph. One samples M points uniformly at random in a volume V and regards them as candidate centers of spheres of diameter D. A graph is then constructed by connecting two points whenever the corresponding spheres overlap. An independent set $\mathcal{I}$ of this graph is a subset of vertices with no edges between them. Therefore, it corresponds to a subset of candidate centers whose spheres do not overlap, and hence defines a valid sphere packing.

Let $|\mathcal{I}|$ be the size of the independent set, and define its relative size by

$$\alpha = \frac{|\mathcal{I}|}{M}. \tag{A1}$$

The expected degree of the geometric graph is

$$K = \frac{M}{V} v_d(D), \tag{A2}$$

up to boundary corrections. The packing fraction associated with the independent set is

$$\varphi = \frac{|\mathcal{I}|}{V} v_d\left(\frac{D}{2}\right). \tag{A3}$$

Using $v_d(D) = 2^d v_d(D/2)$, we obtain the relation

$$K = \frac{2^d \varphi}{\alpha}. \tag{A4}$$

If the random geometric graph behaved as an Erdős–Rényi random graph with average degree K, a greedy algorithm, or a randomized greedy procedure such as the Rödl nibble method, would construct an independent set of relative size

$$\alpha_{\mathrm{alg}} \simeq \frac{\log K}{K}, \tag{A5}$$

up to subleading corrections [46, 47]. By contrast, the maximum independent set of an Erdős–Rényi random graph has the larger asymptotic size

$$\alpha_{\mathrm{MIS}} \simeq \frac{2\log K}{K}. \tag{A6}$$

Thus, even for ordinary random graphs, there is a factor-of-two gap between the size reached by known local constructive algorithms and the maximum independent-set size.

In a random geometric graph, however, edges are not independent. Nearby vertices induce strong local correlations among edges, and it is therefore nontrivial whether the random-graph estimate Eq. (A5) remains attainable. The main

achievement of CJMS is to show that this algorithmic scaling does remain attainable for high-dimensional geometric graphs in a regime where the average degree grows as

$$K = A\left(\frac{d}{\log d}\right)^{d/2}, \tag{A7}$$

with A independent of d. Combining Eqs. (A4), (A5), and (A7), we find, at the level of leading asymptotics,

$$\varphi_{\rm alg} = \frac{\alpha_{\rm alg} K}{2^d} \simeq \frac{\log K}{2^d} \simeq \frac{d\log d}{2^{d+1}}. \tag{A8}$$

This is precisely the density scale of the dynamical transition obtained in the present dissociation replica liquid theory.

The factor-of-two gap between $\alpha_{\rm alg}$ and $\alpha_{\rm MIS}$ also provides a useful heuristic interpretation of the ideal-glass transition. If a geometric analogue of the maximum-independent-set scale $\alpha_{\rm MIS} \simeq 2\log K/K$ were attainable, the corresponding packing fraction would be

$$\varphi_{\rm MIS} = \frac{\alpha_{\rm MIS} K}{2^d} \simeq \frac{2\log K}{2^d} \simeq \frac{d\log d}{2^d}. \tag{A9}$$

This has the same leading scale as the ideal-glass transition density φ_K and the glass close packing density φ_{GCP} predicted by the replica liquid theory [21]. This comparison suggests that the difference between the CJMS lower bound and φ_K or φ_{GCP} may be interpreted heuristically as an algorithmic gap: constructive random packing procedures reach the independent-set scale $\log K/K$, whereas the thermodynamic threshold corresponds to the larger scale $2\log K/K$.

Appendix B: More general ansatz

In the main text, we analyzed the model within the binomial ansatz. In this Appendix, we show that the resulting thermodynamic glass transition is unchanged within a broader class of ansätze. Following the treatment of the hard-core lattice gas on random graphs [48], we consider

$$g(\overline{\mu}) = \int dh\, P(h)\, \frac{\exp\left(h\sum_{a=1}^{m}\mu^a\right)}{(1+e^h)^m}. \tag{B1}$$

Introducing

$$x = \frac{e^h}{1+e^h}, \tag{B2}$$

this ansatz can be rewritten as

$$g_k = \int_0^1 dx\, p(x)\, x^{k-1}(1-x)^{m-k}, \tag{B3}$$

where

$$p(x) \equiv xP(h)\frac{dh}{dx}. \tag{B4}$$

The normalization condition gives

$$\int_0^1 dx\, p(x) = 1. \tag{B5}$$

Thus, $p(x)$ can be interpreted as the probability distribution of the local occupation probability x. The set of all probability distributions $p(x)$ is convex: if $p_1(x)$ and $p_2(x)$ are probability distributions, then $p_\lambda(x) = \lambda p_1(x) + (1-\lambda)p_2(x)$, $0 \le \lambda \le 1$ is also a probability distribution. The binomial ansatz used in the main text corresponds to an extreme point of this convex set,

$$p(x) = \delta(x - x_0). \tag{B6}$$

Within this dissociation ansatz, the ideal-gas contribution is

$$-\beta f^{\rm id} = \frac{d}{2}\log d \int_0^1 dx\, p(x) \left[\frac{1-(1-x)^m}{x} - 2m\right]. \tag{B7}$$

The excess contribution is

$$-\beta f^{\rm ex} = \frac{d\log d}{2}\widetilde{\varphi}\int_{-\infty}^0 dh\, e^h \int_0^1 dx\, dy\, p(x)p(y) \left[\frac{\left\{1+\left(e^{-\tilde{\beta}\tilde{v}(h)}-1\right)xy\right\}^m - 1}{xy}\right]. \tag{B8}$$

Then, the configurational entropy is obtained as

$$\tilde{\Sigma}[p] = \int_0^1 dx\, p(x)A(x) - \widetilde{\varphi}\int_{-\infty}^0 dh\, e^h B(h) \int_0^1 dx\, dy\, p(x)p(y)A(B(h)xy)\,, \tag{B9}$$

where

$$A(x) = 1 + \frac{(1-x)\log(1-x)}{x} = \sum_{n=1}^{\infty}\frac{x^n}{n(n+1)}, \tag{B10}$$

$$B(h) = 1 - e^{-\tilde{\beta}\tilde{v}(h)}. \tag{B11}$$

For a repulsive interaction, $0 \le B(h) \le 1$.

We now show that allowing a distribution $p(x)$ cannot lower the configurational entropy below the result obtained within the binomial ansatz. First, $\tilde{\Sigma}[p]$ is a concave functional of $p(x)$. Indeed, for

$$p_\lambda(x) = \lambda p_1(x) + (1-\lambda)p_2(x), \qquad 0 \le \lambda \le 1, \tag{B12}$$

one finds

$$\tilde{\Sigma}[p_\lambda] - \lambda\tilde{\Sigma}[p_1] - (1-\lambda)\tilde{\Sigma}[p_2] = \widetilde{\varphi}\int_{-\infty}^0 dh\, e^h \sum_{n=1}^{\infty}\frac{B(h)^{n+1}}{n(n+1)}\lambda(1-\lambda)\left(\langle x^n\rangle_1 - \langle x^n\rangle_2\right)^2 \ge 0, \tag{B13}$$

where

$$\langle x^n\rangle_i = \int_0^1 dx\, p_i(x)x^n \qquad (i=1,2). \tag{B14}$$

The concavity of $\tilde{\Sigma}[p]$ suggests, in accordance with Bauer's maximum principle, that the global minimum should be realized at an extreme point of the convex set of probability measures, $p(x) = \delta(x - x_{\rm min})$ [49]. Below we verify this conclusion directly for the present functional. To this end, we define

$$\tilde{\Sigma}(x) = A(x) - \widetilde{\varphi}\int_{-\infty}^0 dh\, e^h B(h) A\big(B(h)x^2\big)\,, \tag{B15}$$

which is precisely the configurational entropy obtained from the binomial ansatz. Then

$$\begin{aligned}
&\tilde{\Sigma}[p] - \int_0^1 dx\, p(x)\tilde{\Sigma}(x) \\
&= \widetilde{\varphi}\int_{-\infty}^0 dh\, e^h B(h)\left[\int_0^1 dx\, p(x)A\big(B(h)x^2\big) - \int_0^1 dx\, dy\, p(x)p(y)A(B(h)xy)\right] \\
&= \widetilde{\varphi}\int_{-\infty}^0 dh\, e^h \sum_{n=1}^{\infty}\frac{B(h)^{n+1}}{n(n+1)}\left[\big\langle x^{2n}\big\rangle - \langle x^n\rangle^2\right] \ge 0.
\end{aligned} \tag{B16}$$

The last inequality follows from the positivity of the variance,

$$\big\langle x^{2n}\big\rangle - \langle x^n\rangle^2 \ge 0. \tag{B17}$$

Therefore,

$$\tilde{\Sigma}[p] \geq \int_0^1 dx\, p(x)\tilde{\Sigma}(x) \geq \min_{0\leq x\leq 1} \tilde{\Sigma}(x). \tag{B18}$$

Hence the global minimum of the configurational entropy within the dissociation ansatz is identical to that obtained within the binomial ansatz. Consequently, the thermodynamic glass transition discussed in the main text is unchanged by allowing fluctuations of the local occupation probability x.

We finally comment on the dynamical transition point. Since $\tilde{\Sigma}[p]$ is concave in p, a metastable minimum associated with the dynamical transition cannot be realized by any non-extreme distribution. Indeed, $\tilde{\Sigma}[p_\lambda]$ can be considered as a one-dimensional concave function of λ, which cannot have a local minimum at an interior point.

Appendix C: Hard-core model on random graphs in the large-degree limit

In this appendix, we discuss the hard-core model on an Erdős–Rényi random graph with mean degree K. The hard-core model on a graph is equivalent to the problem of independent sets: occupied vertices correspond to vertices included in the independent set, and the hard-core constraint forbids two adjacent vertices from being occupied simultaneously. Thus, each allowed configuration of the hard-core model is an independent set of the graph. The purpose of this appendix is to show that, in the large-K limit, the replica free energy of this problem has the same structure as the one obtained for high-dimensional hard spheres in the main text.

1. Settings

We consider a graph $G = (V, E)$ with M vertices. We introduce an occupation variable $\mu_i \in \{0, 1\}$ on each vertex. If $\mu_i = 1$, vertex i is occupied and belongs to the independent set; if $\mu_i = 0$, it is empty. The hard-core constraint requires that no edge connects two occupied vertices. Therefore, the partition function counting independent sets is

$$Z = \sum_{\{\mu_i=0,1\}} \prod_{(ij)\in E} (1 - \mu_i\mu_j). \tag{C1}$$

The factor $(1 - \mu_i\mu_j)$ vanishes when both endpoints of an edge are occupied, and is otherwise equal to one. Hence only independent sets contribute to Z.

We are interested in the entropy of independent sets at fixed density

$$\alpha = \frac{1}{M}\sum_{i=1}^{M} \mu_i. \tag{C2}$$

In the replica calculation below, this density is imposed as a constraint on each replica.

2. Replica free energy

The disorder-averaged free energy is computed from

$$-\beta f = \frac{1}{M}\overline{\log Z} = \lim_{n\to 0} \frac{1}{nM} \log \overline{Z^n}. \tag{C3}$$

The replicated partition function is

$$Z^n = \sum_{\{\mu_i^a=0,1\}} \prod_{(ij)\in E} \prod_{a=1}^{n} (1 - \mu_i^a \mu_j^a). \tag{C4}$$

For an Erdős–Rényi graph in which each edge is present independently with probability K/M, the average over graphs gives [48]

$$\begin{aligned}\overline{Z^n} &= \sum_{\{\mu_i^a=0,1\}} \prod_{i<j} \left[1 - \frac{K}{M} + \frac{K}{M} \prod_{a=1}^{n} (1 - \mu_i^a \mu_j^a)\right] \\ &= \sum_{\{\mu_i^a=0,1\}} \exp\left[-\frac{KM}{2} + \frac{K}{2M} \sum_{ij} \prod_{a=1}^{n} (1 - \mu_i^a \mu_j^a) + O(1)\right]. \end{aligned} \tag{C5}$$

We introduce the replicated order parameter

$$\rho(\overline{\mu}) = \frac{1}{M} \sum_{i=1}^{M} \prod_{a=1}^{n} \delta_{\mu_i^a, \mu^a}, \qquad \overline{\mu} = \{\mu^1, \cdots, \mu^n\}. \tag{C6}$$

It satisfies the normalization condition

$$\sum_{\overline{\mu}} \rho(\overline{\mu}) = 1. \tag{C7}$$

The fixed-density constraint in each replica is

$$\alpha = \sum_{\overline{\mu}} \rho(\overline{\mu}) \mu^a, \qquad a = 1, \cdots, n. \tag{C8}$$

Using the standard saddle-point representation of the order parameter, one obtains

$$\overline{Z^n} = \int D\rho(\overline{\mu}) \exp\left[-M\beta f_n[\rho]\right], \tag{C9}$$

with

$$-\beta f_n[\rho] = -\sum_{\overline{\mu}} \rho(\overline{\mu}) \log \rho(\overline{\mu}) - \frac{K}{2} + \frac{K}{2} \sum_{\overline{\mu},\overline{\nu}} \rho(\overline{\mu}) \rho(\overline{\nu}) \prod_{a=1}^{n} (1 - \mu^a \nu^a). \tag{C10}$$

The free energy should be extremized under the normalization and fixed-density constraints.

3. Factorized 1RSB ansatz

We now consider a one-step replica-symmetry-broken ansatz. The n replicas are divided into n/m blocks of size m, and the order parameter is assumed to factorize over the blocks:

$$\rho(\mu^1, \cdots, \mu^n) = \prod_{r=1}^{n/m} \rho_1(\mu^{(r-1)m+1}, \cdots, \mu^{rm}), \tag{C11}$$

which is tantamount to assuming that m replicas within the block belong to the same glassy metastable state, and that replicas from different blocks are uncorrelated. Substituting this ansatz into Eq. (C10), we obtain

$$\begin{aligned}-\beta f_n = &-\frac{n}{m} \sum_{\overline{\mu}} \rho_1(\overline{\mu}) \log \rho_1(\overline{\mu}) \\ &+ \frac{K}{2} \left[\left(\sum_{\overline{\mu},\overline{\nu}} \rho_1(\overline{\mu}) \rho_1(\overline{\nu}) \prod_{a=1}^{m} (1 - \mu^a \nu^a)\right)^{n/m} - 1\right], \end{aligned} \tag{C12}$$

where now $\overline{\mu} = \{\mu^1, \cdots, \mu^m\}$ is a block variable. Taking the limit $n \to 0$, we find

$$-\beta f = \lim_{n\to 0} \frac{-\beta f_n}{n} = -\frac{1}{m} \sum_{\overline{\mu}} \rho_1(\overline{\mu}) \log \rho_1(\overline{\mu}) + \frac{K}{2m} \log \left[\sum_{\overline{\mu},\overline{\nu}} \rho_1(\overline{\mu}) \rho_1(\overline{\nu}) \prod_{a=1}^{m} (1 - \mu^a \nu^a)\right]. \tag{C13}$$

4. Small-α expansion

In the large-K limit, the density of large independent sets scales as $\alpha = O(\log K/K)$, and is therefore small. We expand Eq. (C13) for $\alpha \ll 1$.

Let $\overline{0}$ denote the empty block, $\mu^a = 0$ for all a. Since the density is small, $\rho_1(\overline{0}) = O(1)$, while $\rho_1(\overline{\mu}) = O(\alpha)$ for $\overline{\mu} \neq \overline{0}$. We write

$$\rho_1(\overline{\mu}) = \delta_{\overline{\mu},\overline{0}}\rho_1(\overline{0}) + (1 - \delta_{\overline{\mu},\overline{0}})\alpha g(\overline{\mu}), \tag{C14}$$

where $g(\overline{\mu}) = \rho_1(\overline{\mu})/\alpha$ for $\overline{\mu} \neq \overline{0}$. The normalization gives

$$\rho_1(\overline{0}) = 1 - \alpha \sum_{|\overline{\mu}|>0} g(\overline{\mu}). \tag{C15}$$

The density constraint becomes

$$\sum_{|\overline{\mu}|>0} g(\overline{\mu})\mu^a = 1, \qquad a = 1, \cdots, m. \tag{C16}$$

Note that removing the $\overline{0}$ in this way precisely correspond to the idea of integrating away ideal gas particles discussed in Sec. IV B. Assuming replica symmetry within each block, $g(\overline{\mu})$ depends only on $|\overline{\mu}| = \sum_{a=1}^m \mu^a$:

$$g(\overline{\mu}) = g_{|\overline{\mu}|}. \tag{C17}$$

Then Eq. (C16) reduces to

$$\sum_{k=1}^{m} \binom{m-1}{k-1} g_k = 1. \tag{C18}$$

The entropic term has the leading small-α behavior

$$\sum_{\overline{\mu}} \rho_1(\overline{\mu}) \log \rho_1(\overline{\mu}) = \alpha \log \alpha \sum_{|\overline{\mu}|>0} g(\overline{\mu}) + O(\alpha). \tag{C19}$$

The interaction term is

$$\begin{aligned} &\log \left[\sum_{\overline{\mu},\overline{\nu}} \rho_1(\overline{\mu})\rho_1(\overline{\nu}) \prod_{a=1}^{m} (1 - \mu^a\nu^a) \right] \\ &\quad = \alpha^2 \sum_{|\overline{\mu}|>0} \sum_{|\overline{\nu}|>0} g(\overline{\mu})g(\overline{\nu}) \left[\prod_{a=1}^{m} (1 - \mu^a\nu^a) - 1 \right] + O(\alpha^3). \end{aligned} \tag{C20}$$

Therefore, to leading order,

$$\begin{aligned} -m\beta f &= -\alpha \log \alpha \sum_{|\overline{\mu}|>0} g(\overline{\mu}) + \frac{K\alpha^2}{2} \sum_{|\overline{\mu}|>0} \sum_{|\overline{\nu}|>0} g(\overline{\mu})g(\overline{\nu}) \left[\prod_{a=1}^{m} (1 - \mu^a\nu^a) - 1 \right] \\ &= -\alpha \log \alpha \sum_{k=1}^{m} \binom{m}{k} g_k - \frac{K\alpha^2}{2} \sum_{k=1}^{m} \binom{m}{k} g_k \sum_{\ell=1}^{k} \sum_{s=0}^{m-k} \binom{k}{\ell} \binom{m-k}{s} g_{\ell+s}. \end{aligned} \tag{C21}$$

This can be identified with the free-energy calculated by the Monasson method [18], since we assumed that the m replicas are in the same glassy metastable state. Equation (C21) has the same functional form as the high-dimensional hard-sphere free energy in the main text, Eq. (32), in the hard-sphere limit $\tilde{\beta} \to \infty$, up to terms linear in m that do not affect the configurational entropy. Note that to obtain a non-trivial results the two terms need to be of the same order, which forces $\alpha \propto \log K/K$ in the independent set problem, and $\varphi \propto d \log d/2^d$ in the hard-sphere model. If these scalings are not respected, the identification does not hold.

5. Binomial ansatz

As in the particle problem, we now impose the binomial ansatz

$$g_k = x^{k-1}(1-x)^{m-k}. \tag{C22}$$

This ansatz satisfies Eq. (C18). Substituting it into Eq. (C21), we obtain

$$-m\beta f = -\alpha \log \alpha \, \frac{1-(1-x)^m}{x} - \frac{K\alpha^2}{2} \frac{1-(1-x^2)^m}{x^2}. \tag{C23}$$

The configurational entropy is obtained by the same Monasson derivative as in the main text. Introducing the rescaled entropy

$$\tilde{\Sigma}(x) \equiv \frac{\Sigma(x)}{-\alpha \log \alpha}, \tag{C24}$$

we find

$$\tilde{\Sigma}(x) = A(x) - \widetilde{\varphi}^{\text{eff}} A(x^2), \tag{C25}$$

where

$$A(x) = 1 + \frac{1-x}{x} \log(1-x), \qquad \widetilde{\varphi}^{\text{eff}} = -\frac{K\alpha}{2\log\alpha}. \tag{C26}$$

Equation (C25) is identical to the hard-sphere configurational entropy in the large-dimensional limit. Therefore, the dynamical and thermodynamic transition points are

$$\widetilde{\varphi}_d^{\text{eff}} = \frac{1}{2}, \qquad \widetilde{\varphi}_K^{\text{eff}} = 1. \tag{C27}$$

Solving these equations for large K gives

$$\alpha_d = \frac{\log K}{K} + O\left(\frac{\log\log K}{K}\right), \qquad \alpha_K = \frac{2\log K}{K} + O\left(\frac{\log\log K}{K}\right). \tag{C28}$$

The second result agrees with the well-known leading asymptotic density of maximum independent sets on large random graphs, while the first gives the corresponding dynamical, or algorithmic, scale. These results are consistent with rigorous results and cavity-method analyses of the hard-core model on random graphs [47, 50]. See Ref. [51] for a comparison of different grand-canonical algorithms for the maximum independent set problem.

[1] P. G. Debenedetti and F. H. Stillinger, Supercooled liquids and the glass transition, Nature **410**, 259–267 (2001).
[2] A. Cavagna, Supercooled liquids for pedestrians, Physics Reports **476**, 51–124 (2009).
[3] L. Berthier and G. Biroli, Theoretical perspective on the glass transition and amorphous materials, Rev. Mod. Phys. **83**, 587 (2011).
[4] T. R. Kirkpatrick and D. Thirumalai, Dynamics of the structural glass transition and the p-spin—interaction spin-glass model, Phys. Rev. Lett. **58**, 2091 (1987).
[5] T. R. Kirkpatrick and P. G. Wolynes, Stable and metastable states in mean-field potts and structural glasses, Phys. Rev. B **36**, 8552 (1987).
[6] E. Leutheusser, Dynamical model of the liquid-glass transition, Phys. Rev. A **29**, 2765 (1984).
[7] U. Bengtzelius, W. Gotze, and A. Sjolander, Dynamics of supercooled liquids and the glass transition, Journal of Physics C: Solid State Physics **17**, 5915–5934 (1984).
[8] T. R. Kirkpatrick and P. G. Wolynes, Connections between some kinetic and equilibrium theories of the glass transition, Physical Review A **35**, 3072 (1987).
[9] T. Maimbourg, J. Kurchan, and F. Zamponi, Solution of the dynamics of liquids in the large-dimensional limit, Phys. Rev. Lett. **116**, 015902 (2016).
[10] G. Szamel, Simple theory for the dynamics of mean-field-like models of glass-forming fluids, Phys. Rev. Lett. **119**, 155502 (2017).

[11] G. Adam and J. H. Gibbs, On the temperature dependence of cooperative relaxation properties in glass-forming liquids, The Journal of Chemical Physics **43**, 139–146 (1965).

[12] T. R. Kirkpatrick, D. Thirumalai, and P. G. Wolynes, Scaling concepts for the dynamics of viscous liquids near an ideal glassy state, Phys. Rev. A **40**, 1045 (1989).

[13] J.-P. Bouchaud and G. Biroli, On the adam-gibbs-kirkpatrick-thirumalai-wolynes scenario for the viscosity increase in glasses, The Journal of Chemical Physics **121**, 7347–7354 (2004).

[14] Y. Singh, J. P. Stoessel, and P. G. Wolynes, Hard-sphere glass and the density-functional theory of aperiodic crystals, Physical Review Letters **54**, 1059 (1985).

[15] T. R. Kirkpatrick and D. Thirumalai, Comparison between dynamical theories and metastable states in regular and glassy mean-field spin models with underlying first-order-like phase transitions, Physical Review A **37**, 4439 (1988).

[16] M. Mezard, G. Parisi, and M. Virasoro, *Spin Glass Theory and Beyond: An Introduction to the Replica Method and Its Applications* (WORLD SCIENTIFIC, 1986).

[17] J.-P. Hansen and I. R. McDonald, *Theory of simple liquids: with applications to soft matter* (Academic press, 2013).

[18] R. Monasson, Structural glass transition and the entropy of the metastable states, Phys. Rev. Lett. **75**, 2847 (1995).

[19] M. Mézard and G. Parisi, A tentative replica study of the glass transition, Journal of Physics A: Mathematical and General **29**, 6515–6524 (1996).

[20] M. Mézard and G. Parisi, Thermodynamics of glasses: A first principles computation, Phys. Rev. Lett. **82**, 747 (1999).

[21] G. Parisi and F. Zamponi, Mean-field theory of hard sphere glasses and jamming, Rev. Mod. Phys. **82**, 789 (2010).

[22] G. Parisi, P. Urbani, and F. Zamponi, *Theory of Simple Glasses: Exact Solutions in Infinite Dimensions* (Cambridge University Press, 2019).

[23] J. Kurchan, G. Parisi, and F. Zamponi, Exact theory of dense amorphous hard spheres in high dimension i. the free energy, Journal of Statistical Mechanics: Theory and Experiment **2012**, P10012 (2012).

[24] J. Kurchan, G. Parisi, P. Urbani, and F. Zamponi, Exact theory of dense amorphous hard spheres in high dimension. ii. the high density regime and the gardner transition, The Journal of Physical Chemistry B **117**, 12979–12994 (2013).

[25] P. Charbonneau, J. Kurchan, G. Parisi, P. Urbani, and F. Zamponi, Exact theory of dense amorphous hard spheres in high dimension. iii. the full replica symmetry breaking solution, Journal of Statistical Mechanics: Theory and Experiment **2014**, P10009 (2014).

[26] M. Sellitto and F. Zamponi, A thermodynamic description of colloidal glasses, EPL (Europhysics Letters) **103**, 46005 (2013).

[27] A. Altieri, P. Urbani, and F. Zamponi, Microscopic theory of two-step yielding in attractive colloids, Physical Review Letters **121**, 10.1103/physrevlett.121.185503 (2018).

[28] H. Ikeda, K. Miyazaki, H. Yoshino, and A. Ikeda, Multiple glass transitions and higher-order replica symmetry breaking of binary mixtures, Physical Review E **103**, 10.1103/physreve.103.022613 (2021).

[29] H. Kim and A. Ikeda, Replica theory for the dynamic glass transition of hard spheres with continuous polydispersity, Phys. Rev. E **111**, 035401 (2025).

[30] M. Campos, M. Jenssen, M. Michelen, and J. Sahasrabudhe, A new lower bound for sphere packing, arXiv:2312.10026 10.48550/arXiv.2312.10026 (2023).

[31] M. Ozawa, A. Ikeda, K. Miyazaki, and W. Kob, Ideal glass states are not purely vibrational: Insight from randomly pinned glasses, Phys. Rev. Lett. **121**, 205501 (2018).

[32] G. Biroli, P. Charbonneau, E. I. Corwin, Y. Hu, H. Ikeda, G. Szamel, and F. Zamponi, Interplay between percolation and glassiness in the random lorentz gas, Physical Review E **103**, L030104 (2021).

[33] G. Jung, M. Ozawa, G. Biroli, and L. Berthier, Numerical investigation of the equilibrium kauzmann transition in a two-dimensional atomistic glass, arXiv:2507.03590 10.48550/arXiv.2507.03590 (2025).

[34] M. Mangeat and F. Zamponi, Quantitative approximation schemes for glasses, Physical Review E **93**, 012609 (2016).

[35] D. Frenkel and A. J. C. Ladd, New monte carlo method to compute the free energy of arbitrary solids. application to the fcc and hcp phases of hard spheres, The Journal of Chemical Physics **81**, 3188–3193 (1984).

[36] F. Sciortino, W. Kob, and P. Tartaglia, Inherent structure entropy of supercooled liquids, Phys. Rev. Lett. **83**, 3214 (1999).

[37] L. Berthier, M. Ozawa, and C. Scalliet, Configurational entropy of glass-forming liquids, The Journal of Chemical Physics **150**, 10.1063/1.5091961 (2019).

[38] A. Ninarello, L. Berthier, and D. Coslovich, Models and algorithms for the next generation of glass transition studies, Physical Review X **7**, 021039 (2017).

[39] H. Ikeda, F. Zamponi, and A. Ikeda, Mean field theory of the swap monte carlo algorithm, The Journal of Chemical Physics **147**, 234506 (2017).

[40] F. Ghimenti, L. Berthier, J. Kurchan, and F. van Wijland, Clever algorithms for glasses work by time reparameterization, Proceedings of the National Academy of Sciences **123**, e2520818123 (2026).

[41] C. Cammarota and G. Biroli, Ideal glass transitions by random pinning, Proceedings of the National Academy of Sciences **109**, 8850 (2012).

[42] M. Ozawa, W. Kob, A. Ikeda, and K. Miyazaki, Equilibrium phase diagram of a randomly pinned glass-former, Proceedings of the National Academy of Sciences **112**, 6914 (2015).

[43] W. A. Phillips, Two-level states in glasses, Reports on Progress in Physics **50**, 1657 (1987).

[44] D. Chandler and J. P. Garrahan, Dynamics on the way to forming glass: Bubbles in space-time, Annual Review of Physical Chemistry **61**, 191–217 (2010).

[45] A. S. Keys, L. O. Hedges, J. P. Garrahan, S. C. Glotzer, and D. Chandler, Excitations are localized and relaxation is hierarchical in glass-forming liquids, Phys. Rev. X **1**, 021013 (2011).

[46] J. B. Shearer, A note on the independence number of triangle-free graphs, Discrete Mathematics **46**, 83–87 (1983).
[47] A. Coja-Oghlan and C. Efthymiou, On independent sets in random graphs, Random Structures & Algorithms **47**, 436 (2014).
[48] M. Weigt and A. K. Hartmann, Minimal vertex covers on finite-connectivity random graphs: A hard-sphere lattice-gas picture, Phys. Rev. E **63**, 056127 (2001).
[49] C. D. Aliprantis and K. C. Border, *Infinite dimensional analysis: a hitchhiker's guide* (Springer, 2006).
[50] J. Barbier, F. Krzakala, L. Zdeborová, and P. Zhang, The hard-core model on random graphs revisited, Journal of Physics: Conference Series **473**, 012021 (2013).
[51] M. C. Angelini and F. Ricci-Tersenghi, Monte carlo algorithms are very effective in finding the largest independent set in sparse random graphs, Physical Review E **100**, 013302 (2019).